Importance of Electronic Delocalization on the C−N Bond Rotation in $HCX(NH_2)$ (X = O, NH, CH_2, S, and Se)

Yirong Mo,*,†,‡ Paul von Ragué Schleyer,§ Wei Wu,‡ Menghai Lin,‡ Qianer Zhang,‡ and Jiali Gao||

Department of Chemistry, Western Michigan University, Kalamazoo, Michigan 49008, Department of Chemistry, State Key Laboratory for Physical Chemistry of Solid Surfaces and Center for Theoretical Chemistry, Xiamen University, Xiamen, Fujian 361005, People's Republic of China, Department of Chemistry, University of Georgia, Athens, Georgia 30602, and Department of Chemistry and Minnesota Supercomputing Institute, University of Minnesota, Minneapolis, Minnesota 55455

Received: August 28, 2003

A block-localized wave function method, which in effect can switch off conventional conjugation and hyperconjugation effects, is employed to investigate the origin of the rotational barriers in formamide and its analogues. It is found that the resonance between the π electrons on the C=X double bond and the nitrogen lone pair significantly stabilizes the planar conformation in $HCXNH_2$ (X = O, NH, CH_2, S, and Se). The absolute resonance energy follows the order of formamide < thioformamide < selenoformamide, with predicted vertical resonance energies of −25.5, −35.7, and −37.6 kcal/mol, respectively. The computed vertical resonance energies for X = O, NH, and CH_2 are −25.5, −22.5, and −19.1 kcal/mol, respectively, which follow the decreasing trend of electronegativity. Although the rotational barrier about the C−N bond in vinylamine (4.5 kcal/mol) is much smaller than that of formamide (15.7 kcal/mol), the resonance energy in vinylamine is of the same order as that of formamide (−19.1 versus −25.5 kcal/mol). Consequently, the rotational barrier in formamide cannot be simply regarded as a result of the carbonyl polarization as proposed in early studies. In fact, energy decomposition results reveal that resonance and σ-framework steric effects are equally important for the estimated difference in rotational barrier. Ab initio valence bond calculations are performed to investigate the electronic delocalization in formamide and its analogues. Examination of the electron density difference between the adiabatic (delocalized) and diabatic (localized) states revealed that the resonance in the planar formamide shifts electron density from nitrogen both to carbon and to oxygen, supporting the conventional resonance model. This is accompanied by the opposing migration of the σ charge density, making the integrated atomic charges smaller than that expected from pure π delocalization.

Introduction

The origin of the nearly planar geometry and the large rotational barrier about the amide bond has been extensively investigated both theoretically and experimentally because the amide bond is the building block of a polypeptide chain.[1] In principle, these experimental observations can be rationalized by the resonance between the nitrogen lone pair and the carbonyl group π system.[2] According to valence bond (VB) theory, the π electronic structure of the amide bond can be described by six resonance structures resulting from four π electrons and three π-type atomic orbitals (Chart 1).

The dashed line in structure **4** indicates spin coupling between electrons in the atomic orbitals on the oxygen and nitrogen atom. Contribution from resonance structure **3**, which contains a formal double bond between carbon and nitrogen, is considered to be primarily responsible for the planar structure and the high rotational barrier about the amide bond.[3] Resonance structure **3** also implies that there is significant charge delocalization from the nitrogen lone pair to the carbonyl oxygen.

CHART 1

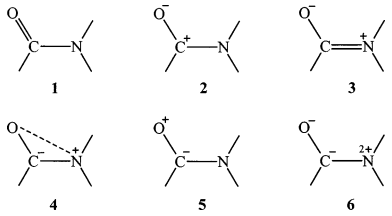

Despite these insightful features, the validity of the VB resonance model for the simplest amide, formamide, has been challenged on the basis of population analyses, using the atoms-in-molecules (AIM) theory.[4] Wiberg and co-workers[5,6] found that the charge population on the carbonyl oxygen is essentially unchanged as a function of the torsional angle about the amide bond. This led Wiberg and co-workers to suggest that the charge variation mainly occurs on the amide nitrogen and the carbonyl carbon with little involvement of the oxygen atom in the C−N bond rotation, in contrast to that suggested by resonance structure **3**.[5−7] Furthermore, in accord with Wiberg's results, Knight and Allen[8] showed that the rotational barrier of formamide could be rationalized by changes in the C−N bond energy alone by a one-electron valence energy decomposition analysis.

† Western Michigan University.
‡ Xiamen University.
§ University of Georgia.
|| University of Minnesota.

10.1021/jp036560c CCC: $25.00
Published on Web 10/29/2003

Interestingly, Wiberg and Rablen[7] subsequently extended their work to thioamides and the series of $HCX(NH_2)$, where X = NH, PH, CH_2, and SiH_2, and suggested that the charge patterns are consistent with the traditional VB picture. However, Laidig and Cameron[9,10] argued that the origin of the barrier to amide rotation in thioamides is due to the intrinsic preference of the amide nitrogen for planarity, making it more electronegative and better stabilized.

In contrast, Fogarasi and Szalay[11] provided compelling evidence supporting the amide resonance model by analyzing geometric change, charge variation, and NMR data as a function of the torsional angle. Similarly, Glendening and Hrabal[12] performed natural atomic orbital (NAO)[13] population analysis on formamide and its chalcogen analogues, revealing strong resonance stabilization in the planar geometry. Lauvergnat and Hiberty[14] pointed out that previous conclusions were obtained on the basis of indirect evidence, such as population analyses or group separation reactions. Although electronic delocalization may be reflected by the change of charge distribution, it is often complicated by the opposing effects of σ and π electrons.[5] Therefore, a quantitative measure of the resonance effect must be obtained by computing the delocalization energy of π electrons. Lauvergnat and Hiberty probed the validity of the resonance model for formamide and thioformamide using an ab initio VB method,[14] which allows the electronic delocalization in these two molecules to be "turned on" or "turned off".[14−16] The electronic delocalization energies are determined by comparing the fully delocalized (adiabatic) ground state and the localized, diabatic state, in which the nitrogen lone pair is constrained to remain localized.[14] Although the results are convincing, a shortcoming of that study is that only electrons of the nitrogen lone pair are localized, whereas the π electrons in the carbonyl group are delocalized over the entire molecule.[14] The effect of the electronic delocalization in the rotamer conformation was not explored. Furthermore, only the negative hyperconjugation effect was considered, whereas the hyperconjugation interaction between the amino group π_{NH_2} electrons and $\pi_{C=O}$* orbital was neglected.[14]

In this study, we investigate the VB resonance model for formamide using the block-localized wave function (BLW) method that was developed recently.[17] The BLW method allows the π electrons in the carbonyl group to be effectively localized in addition to the localization of the nitrogen lone pair. In addition, ab initio VB calculations[15,18,19] are performed to investigate quantitative contributions of the individual resonance structures **1**−**6** to the stabilization of the planar geometry of formamide, HC═NH(NH_2), and HC═CH_2(NH_2). Specific energy components of the overall rotational barrier about the amide bond in $HCX(NH_2)$, where X = O,[5−12,14,20] NH, CH_2, S,[7,10,12,14,21] and Se,[22] are analyzed.

Methods

Electronic delocalization is concerned with interactions between occupied molecular orbitals (MOs) of a molecular fragment and unoccupied molecular orbitals of other fragments. In Hartree−Fock (HF) theory, molecular orbitals are expanded over all primitive atomic orbitals (AOs) and are thus delocalized. The localized MOs obtained from canonical MOs via unitary transformation are not strictly localized on bonds (or lone pairs). These localized MOs contain a mixture of orthogonalization and delocalization tails. Unfortunately, there is no unique way to discriminate these two types of tails. Thus, methods that are based on various localization schemes can yield very different results on delocalization energy and resonance effects.

To circumvent this problem, we construct the wave function for a hypothetical and strictly localized structure (diabatic state) by removing both orthogonalization and delocalization tails in the very beginning. The block-localized wave function (BLW), Ψ^{BLW}, is defined with the assumption that all electrons and primitive basis functions in a molecule can be divided into subgroups.[17] In Ψ^{BLW}, each MO is restricted to be expanded in a subgroup of the basis functions. The Slater determinant wave function for a particular resonance structure or a subset of VB configurations, *g*, is then constructed as

$$\Psi_g = \hat{A}(\Phi_1\Phi_2...\Phi_{k_g}) \tag{1}$$

where $\hat{A}$ is an antisymmetrizing operator, k_g is the number of electronic blocks (subgroups), and Φ_a is a successive product of the occupied MOs in the *a*th subgroup:

$$\Phi_a = \varphi_1^a\alpha\varphi_1^a\beta\varphi_2^a\alpha...\varphi_{n_a/2}^a\beta \tag{2}$$

where α and β are spin functions, n_a is the number of electrons in the *a*th subgroup, and the MOs φ_i^a are linear combinations of atomic orbitals in subgroup *a*. The wave function defined in eq 1 is subjected to the restriction that molecular orbitals within each subgroup are orthogonal, whereas orbitals between different subgroups are nonorthogonal—a feature of the valence bond approach.

The energy difference between the Hartree−Fock wave function Ψ^{HF} and the BLW wave function Ψ^{BLW} can be defined as the electronic delocalization energy, or, resonance energy E_{res}:[17]

$$E_{res} = E(\Psi^{HF}) - E(\Psi^{BLW}) \tag{3}$$

where $E(\Psi^{HF})$ and $E(\Psi^{BLW})$ are the HF and BLW electronic energy, respectively. A comparison between electron densities determined from Ψ^{HF} and Ψ^{BLW} will, therefore, manifest how resonance interactions redistribute the electron population in the system.

In formamide and the analogous series, $HCX(NH_2)$, where X = O, NH, CH_2, S, and Se, the electrons and primitive orbitals are partitioned into three blocks. The first block includes the π electrons in the C═X group, the second block contains the nitrogen lone pair, and the remaining electrons and orbitals form the third block. The third block is also labeled as the σ-framework for simplicity. For the planar formamide, the wave functions for the adiabatic (or delocalized) and the diabatic (or localized) states are expressed as

$$\Psi_g^{HF} = \hat{A}(\sigma\mathbf{1a''^2 2a''^2}) \tag{4}$$

$$\Psi_g^{BLW} = \hat{A}(\sigma\pi_{\mathbf{CO}}^{\ 2}\mathbf{n}_{\mathbf{N}}^{\ 2}) \tag{5}$$

where the subscript g indicates the ground-state planar structure, the superscripts HF and BLW specify the Hartree−Fock and block-localized wave functions, 1a″ and 2a″ are canonical molecular orbitals, primarily composed of the carbonyl π bond and the nitrogen lone pair orbital, and π_{CO} and n_N represent the strictly localized carbonyl π bond and the nitrogen lone pair orbital in the BLW scheme. The symbol σ represents the rest of the molecular orbitals of the σ-framework of the molecule. It should be emphasized that σ, π_{CO}, and n_N in eq 5 are nonorthogonal in the BLW method, and the σ orbitals in the HF and BLW treatment (eqs 4 and 5) are not necessarily identical.

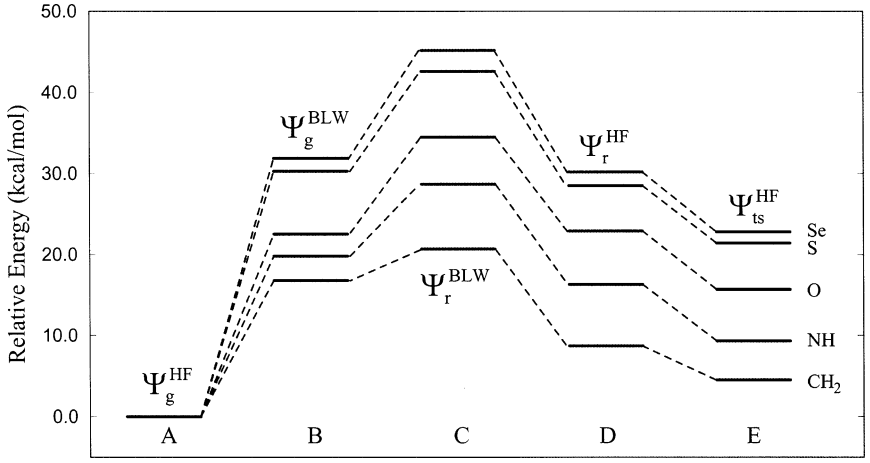

Figure 1. Schematic representation of the energy components contributing to the overall rotational barrier about the C−N bond in $HCXNH_2$ where X = O, S, Se, NH_2, and CH_2.

Similarly, the delocalized and localized wave functions for the 90° rotamer conformation of formamide about the C−N bond are given as follows:

$$\Psi_r^{HF} = \hat{A}(\sigma 2a''^2 10a'^2) \quad (6)$$

$$\Psi_r^{BLW} = \hat{A}(\sigma \pi_{CO}^2 n_N^2) \quad (7)$$

where the subscript r indicates the 90° rotamer structure. For the planar conformation, the definition of Ψ^{BLW} in eq 5 implies that only a mixture of resonance structures **1**, **2**, and **5** are taken into account, which is in contrast to the HF wave function, where all six resonance structures **1**−**6** are implicitly included. In the 90° rotamer conformation, either the first or the second block can be combined with the third block to result in a new BLW with two blocks, which can be used to evaluate the positive and negative hyperconjugation effects individually (see below).

To provide additional insight, the rotational barriers in $HCXNH_2$ are decomposed in terms of resonance conjugation, "steric" effects, hyperconjugation, and pyramidalization. The molecular geometries used in the decomposition scheme in Figure 1 are determined as described below:

1. The planar geometry, A, is optimized at the HF/6-31G(d) level. The planar conformation is the ground state for formamide, thioformamide, and selenoformamide, whereas vinylamine and formamidine have a pyramidal geometry for the amino group. However, the two planar structures in these cases are only 0.5 and 1.7 kcal/mol higher in energy, respectively, and thus are used in the energy decomposition analysis. Deactivation of the π electron conjugation yields a strictly localized structure, B, which is optimized by the BLW method. The energy change, $-\Delta E_R$, from A to B is the adiabatic resonance energy (ARE).[15,24]

2. Rotation about the C−N bond by 90° in the BLW approach yields structure C, which is still an electronically localized structure. Thus, the rotation from structure B to structure C represents purely σ bond rotation without resonance effects. Since π electronic delocalization is absent in B and C, the energy change, ΔE_σ, arises mainly from electronic repulsion between the carbonyl and amino group. Thus, it may be ascribed as "steric" effects.

3. Allowing electronic delocalization in C leads to structure D, which is obtained from constrained optimization at the HF/6-31G(d) level by keeping the amino group planar with a dihedral angle of 90° to the carbonyl plane. The energy variation in this step, ΔE_H, is ascribed to the hyperconjugation effect.

TABLE 1: Computed Vertical Resonance Energies of the Planar $HCXNH_2$ Species[a]

	BLW		ab initio VB
X	6-31G(d)	6-311G(d,p)	6-31G(d)
O	−25.5	−26.0	−24.6
NH	−22.5	−23.1	−20.8
CH_2	−19.1	−19.7	−17.0
S	−35.7	−36.2	
Se	−37.6	−38.3	

[a] Vertical resonance energies (VREs) were computed by the block-localized wave function (BLW) method and ab initio valence bond theory and are given in kilocalories per mole.

4. Relaxation of the geometrical constraints on the NH_2 group in configuration D results in the pyramidal transition structure E, with pyramidalization stabilization energy ΔE_P. Structure E is obtained by HF/6-31G(d) optimization without any constraints. There are two transition structures corresponding to the syn and anti conformations between the carbonyl group and the nitrogen lone pair.[1e,f,7] The syn conformation is slightly lower in energy in all cases except vinylamine, in which the anti transition structure is 1.3 kcal/mol more stable. Consequently, we choose to use the syn conformer in this analysis.

The overall rotational barrier ΔE_b is the sum of these four energy terms.

Results and Discussion

Resonance Effects. The extent of π conjugation in the planar amide structure is most directly related to the vertical resonance energy (VRE), which is the energy change in going from the fully delocalized ground state (HF) to the localized, diabatic (BLW) electronic configuration at the optimized ground-state HF/6-31G(d) geometry.[14,15] Table 1 lists the computed VRE along with the results obtained from ab initio VB calculations (Appendix A). In the latter study, only $HCXNH_2$ (X = O, CH_2, and NH) were considered using the 6-31G(d) basis set.[15,18] We note that the *one-electron atomic orbital* in VB calculations consists of only atomic orbitals on a particular atom, which is determined self-consistently for each resonance structure. This "classical" VB approach differs from "modern" ab initio VB theory, in which the one-electron orbitals are extended to more than one atom and are thus polarized due to mixing with orbitals on other atoms. The structural weights (see Appendix A for definition) of the six resonance structures are listed in Table 2, which provide an indication of the relative contributions of individual resonance structures to the delocalized state. In the

TABLE 2: Computed Structural Weight at the Ab Initio Valence Bond Level by Use of the 6-31G(d) Basis Set

	X = O		X = NH		X = CH_2	
structure	6 VB conf	3 VB conf	6 VB conf	3 VB conf	6 VB conf	3 VB conf
1	0.461	0.601	0.545	0.677	0.611	0.725
2	0.318	0.366	0.246	0.268	0.190	0.196
3	0.131		0.098		0.070	
4	0.065		0.070		0.069	
5	0.023	0.033	0.041	0.055	0.061	0.079
6	0.002		0.001		0.000	

ab initio VB calculation, vertical resonance energies are determined by taking the energy difference between VB energies that is determined with the inclusion of all six resonance configurations and that consisting of only three VB structures, **1**, **2**, and **5**. The latter three resonance structures describe the π_{CO} bond polarization, which are implicitly included in the π_{CO} block in the BLW theory (eq 5). This treatment makes the ab initio VB results directly comparable with the BLW values.

The vertical resonance energies from ab initio VB calculations are −24.6, −20.8, and −17.0 kcal/mol for $HCXNH_2$, where X = O, NH, and CH_2, respectively. This may be compared with the corresponding BLW values of −25.5, −22.5, and −19.1 kcal/mol at the HF/6-31G(d) level (Table 1) and of −26.0, −23.1 and −19.7 kcal/mol at the HF/6-311G(d,p) level. The agreement between results from the ab initio VB and the BLW methods is good. Furthermore, there is minimal dependence on the basis function used in the BLW calculations. Interestingly, much greater delocalization energies are obtained for thioformamide and selenoformamide with estimated values of −35.7 and −37.6 kcal/mol from BLW calculations. Using an alternative ab initio valence bond approach, Lauvergnat and Hiberty[14] reported a vertical resonance energy of −27.3 kcal/mol for formamide and −37.6 kcal/mol for thioformamide with the 6-311++G(d,p) basis set. For comparison, resonance energies of −25.1, −48.4, and −51.4 kcal/mol were obtained for the X = O, S, and Se series from natural resonance theory.[12] Notice that the values for thioformamide and selenoformamide are much greater than the BLW and ab initio VB data.

The contribution of individual resonance structures to the ground-state delocalization is reflected by the VB structural weights for the planar $HCXNH_2$ (X = O, NH, and CH_2) species (Table 2). The covalent configuration, **1**, makes the largest contribution, followed by significant dipolar polarization from **2** in the C=X π bond. Covalent characters increase with decreasing electronegativity of X, which is concomitantly accompanied by decrease in the ionic feature of **2**. Structure **3**, which is responsible for the partial double-bond character in the amide bond, contributes, respectively, 13%, 10%, and 7% to the ground-state charge delocalization of formamide, formamidine, and vinylamine. This is nicely mirrored by the computed vertical resonance energy for these compounds, which descends in that order (Table 1). The relatively large structural weight for structure **3** suggests that it is essential to include this configuration to adequately describe the π conjugation of the amide bond, especially for formamide. Similar conclusions were obtained by Lauvergnat and Hiberty.[14]

Early calculations often included resonance structures **1** and **3** only in VB theory. Pauling estimated that these two resonance structures contribute 60% and 40%, respectively, to the ground-state energy of formamide.[2a] Using the natural resonance theory (NRT) at the MP2/6-31+G(d) level, Glendening and Hrabal[12] found that the structural weights for the covalent (**1**) and dipolar resonance (**3**) forms are 58.6% and 28.6% with other minor contributions. However, in that study, the one-electron orbitals are not strictly atomic orbitals, where the basis set polarization can lead to the mixing of other Lewis resonance structures. Thus, the "dipolar" state is not purely structure **3** but it is a mixture of **2**, **3**, and **6**.

In the chalcogen group, the degree of π electronic delocalization from the nitrogen lone pair into the carbonyl group increases in the order of decreasing electronegativity: formamide < thioformamide < selenoformamide, a counterintuitive observation that has been discussed previously.[7,12,14] Through natural bond orbital analysis, Glendening and Hrabal suggested that the higher polarizability of the heavier chalcogen facilitates the reverse π^*_{CX} polarization, leading to enhanced delocalization from the neighboring nitrogen lone pair. This is consistent with the natural atomic orbital (NAO) population at the nitrogen atom (see Supporting Information), which decreases in the same order as the increase in resonance energy: $HCONH_2$ (1.810 e) > $HCSNH_2$ (1.726 e) > $HCSeNH_2$ (1.707 e).

Rotational Barrier about the C−N Bond. To understand the origin of the large rotational barrier about the C−N bond in formamide and the chalcogen analogues relative to the X = NH and CH_2 species, we decompose the overall torsional energy into four specific components, including resonance delocalization (ΔE_R), σ rotation or "steric" effects (ΔE_σ), hyperconjugation stabilization (ΔE_H), and pyramidization energy (ΔE_P). The procedure, which is similar to that used by Lauvergnat and Hiberty, is illustrated in Figure 1. The quantitative values of the ΔE_R term are different from the vertical resonance energies listed in Table 1 because geometries are reoptimized for the charge-localized or diabatic state. Thus, the ΔE_R term corresponds to the *adiabatic resonance energy*. The ΔE_R contribution to the total torsional barrier may be regarded as a ground-state effect since it is concerned with the planar π electron delocalization in the ground-state structure. The relative energy of the 90° rotamer about the C−N bond includes two contributing factors: (1) the conformational energy of the σ framework, ΔE_σ, which is of "steric" origin, and (2) the difference in hyperconjugation effects, ΔE_H. Hybridization of the amino group into a pyramidal structure provides additional stabilization to the transition structure, which is represented by the ΔE_P term. These energy changes correspond, respectively, to energy differences specified by dashed lines in Figure 1 from configuration A through configuration E.

The computed rotational barriers of $HCXNH_2$ (X = O, NH, CH_2, S, and Se) about the amide bond are 15.7, 9.3, 4.5, 21.4, and 22.8 kcal/mol, respectively, at the HF/6-31G(d) level. These may be compared with values obtained previously at different levels of theory. For X = O, S, and Se, the computed barriers are 16.1, 21.0, and 22.8 kcal/mol at the HF/6-31+G(d) level and 17.2, 19.5, and 20.4 kcal/mol at the MP2/6-31+G(d) level. The rotational barriers of formamide and thioformamide are 16.0 and 18.0 kcal/mol from the G2 theory. Thus, the HF/6-31G(d) values are in reasonable agreement with higher level results and are appropriate for the present energy decomposition analysis.

Listed in Table 3 are energy components that make contributions to the overall rotational barrier (Figure 1). The π electronic delocalization is the predominant factor governing the torsional barrier in these compounds, which largely determines the difference in the computed torsional barrier for the $HCXNH_2$ series. A further contribution results from the rotation about the C−N "single" bond because the resonance effect due to π electron delocalization has been "turned off" in this step. Charge delocalization through hyperconjugation at the 90° rotamer conformation, which is further analyzed in the next section,

TABLE 3: Individual Energy Contributions to the Total Torsional Barrier about the C−N Bond in $HCX(NH_2)$ Molecules[a]

X	ΔE_R	ΔE_σ	ΔE_H	ΔE_P	ΔE_b	$\Delta\Delta E_b$
O	22.5	12.0	−11.6	−7.2	15.7	0.0
NH	19.8	8.9	−12.4	−7.0	9.3	−6.4
CH_2	16.8	3.9	−12.0	−4.2	4.5	−11.2
S	30.3	12.3	−14.1	−7.1	21.4	5.7
Se	31.9	13.3	−15.0	−7.4	22.8	7.1

[a] All energies are obtained by use of the 6-31G(d) basis set and are given in kilocalories per mole.

TABLE 4: Computed Hyperconjugation, Negative Hyperconjugation, and Total Stabilization Energies for the 90° Rotamer Structure of $HCX(NH_2)$ Species[a]

X	$\Delta E_{PH}(\pi_{NH_2} \rightarrow \pi_{CX}^*)$	$\Delta E_{NH}(n_N \rightarrow \sigma_{CX}^*)$	$\Delta E_{PH} + \Delta E_{NH}$	ΔE_{tot}
O	−4.9	−8.1	−13.0	−13.1
NH	−5.5	−8.5	−14.0	−14.1
CH_2	−5.7	−7.9	−13.6	−13.6
S	−6.6	−9.6	−16.2	−16.4
Se	−6.7	−10.6	−17.3	−17.4

[a] All energies are obtained by use of the 6-31G(d) basis set and are given in kilocalories per mole.

along with pyramidization stabilization of the amino group compensate for the destabilization effect to yield the overall rotation barrier. The difference in ground-state resonance effects raises the barrier heights for X = S and Se by 7.8 and 9.4 kcal/mol relative to formamide. These are reduced slightly by the greater hyperconjugation effects in the rotamer structures, giving rise to a net electronic delocalization contribution of 5.3 and 6.0 kcal/mol to the overall $\Delta\Delta E_b$ (5.7 and 7.1 kcal/mol) for X = S and Se. Steric factors and pyramidization of the amino group only makes modest contributions of 0.4 and 1.1 kcal/mol to the relative barrier height $\Delta\Delta E_b$ in $HCSNH_2$ and $HCSeNH_2$ with respect to formamide. On the other hand, both ground-state resonance effects and steric interactions are critical for the progressive decrease in torsional barrier in the series, $HCXNH_2$, where X = O, NH, and CH_2. Furthermore, ground-state resonance effects are smaller in X = NH and CH_2 than in formamide, which contributes to the *reduction* in torsional barrier by 2.7 and 5.7 kcal/mol relative to that of formamide, in contrast to the chalogen series, where the ΔE_R term makes positive contributions. Hyperconjugation effects have similar stabilizing contributions in all 90° rotamers, thereby having little effect on the difference in torsional barrier. Steric effects in the σ-framework are more important for these compounds, which further lowers the barrier height by 3.1 and 8.1 kcal/mol for HC═NH(NH_2) and HC═CH_2(NH_2). The large contribution of the ΔE_σ term may be attributed to the change in basicity of the X group in $HCX(NH_2)$ in going from O to NH and to CH_2, affecting interactions with the amino group in the planar structure. In the $HCXNH_2$ (X = O, NH, and CH_2) series, it is the combination of resonance and steric effects that is largely responsible for the differential barriers.

Hyperconjugation Effects in the 90° Rotamer. The hyperconjugation effects in the 90° rotamer structure are further analyzed by examining individual energy contributions. Here, we use the vertical hyperconjugation energy in the analysis, which is slightly different than the values (ΔE_H) listed in Table 4 because they are the adiabatic delocalization energies having geometry variations included. There are two types of hyperconjugation interactions in the 90° rotamer conformation that affect the energy of the rotational barrier (see Figure 3). The first is the "positive" hyperconjugation interaction between the $\pi_{C=X}^*$ orbital and the antisymmetric combination of the two σ_{NH} orbitals (i.e., π_{NH_2}). The second type refers to the negative hyperconjugation[29] of the nitrogen lone pair electrons and the σ^* orbital of the C═X bond, which may also be considered as anomeric effect. It may be noted that interactions between the oxygen lone pair and the σ_{CN}^* orbital in formamide do not affect the energy of the C−N bond rotation. The hyperconjugation stabilization energy of the first type, $\Delta E_{PH}(\pi_{NH_2} \rightarrow \pi_{C=X}^*)$ can be determined by localizing the π electrons and atomic orbitals with π symmetry on the C═X group. The stabilization energy due to the negative hyperconjugation effect, $\Delta E_{NH}(n_N \rightarrow \sigma_{CX}^*)$, is evaluated by localizing the nitrogen lone pair orbital. The total vertical hyperconjugation energy is the sum of $\Delta E_{PH}(\pi_{NH} \rightarrow \pi_{C=X}^*)$ and $\Delta E_{NH}(n_N \rightarrow \sigma_{CX}^*)$, which can also be computed by a three-block BLW calculation, ΔE_{tot} (Table 4), where the C═X π electrons, the nitrogen lone pair, and the remaining electrons and atomic orbitals are localized.

The computed hyperconjugation energies for the 90° rotamer are listed in Table 4. As expected, the sum of $\Delta E_{PH}(\pi_{NH_2} \rightarrow \pi_{C=X}^*)$ and $\Delta E_{NH}(n_N \rightarrow \sigma_{CX}^*)$ is indeed similar to the total hyperconjugation energy from Ψ^{HF} and Ψ^{3BLW} calculations, ΔE_{tot}(3-BLW), suggesting that the two types of hyperconjugation effects are additive in these molecules as expected based on symmetry. For the oxygen group, both $\Delta E_{PH}(\pi_{NH_2} \rightarrow \pi_{C=X}^*)$ and $\Delta E_{NH}(n_N \rightarrow \sigma_{CX}^*)$ increase in the O, S, and Se series. However, for elements of the same row (X = O, NH, and CH_2), similar total hyperconjugation effects are found for all three systems. Overall, the negative hyperconjugation effect is more pronounced than that of the positive hyperconjugation.[27]

Electron Density Difference Map. In principle, charge population analysis can provide valuable information about electronic delocalization and resonance. The difficulty in practice, however, is that the charge population is not uniquely defined and depends on the method used in the analysis.[30] Thus, it is instructive to compare the electron density of the adiabatic state (Ψ^{HF}) with the corresponding diabatic state (Ψ^{BLW}). The change of the electron density itself, which is a physical observable, provides direct indication of the direction of electronic delocalization in a molecular system.[31] In particular, the electron density difference (EDD) map is defined as follows:

$$\Delta\rho(\vec{r}) = \rho^{HF}(\vec{r}) - \rho^{BLW}(\vec{r}) \tag{8}$$

where ρ^{HF} and ρ^{BLW} are electron densities at position $\vec{r}$ computed from the HF and BLW wave function, respectively.

The EDD plot, illustrating the resonance between the nitrogen lone pair and the C═O π electrons for formamide, is depicted in Figure 2. Here, dashed contours, representing decrease in electron density, are primarily localized in the p_π orbital region of nitrogen, whereas solid contours, specifying increase in charge density, dominate the C═O π orbital. Thus, the flow of electrons of the nitrogen lone pair into the C═O π^* orbital is vividly reflected in the EDD map. Interestingly, the σ electron density migrates concomitantly in the opposite direction from the C−O σ bond toward the amino group to offset the π electron delocalization. The same trends of charge flow are observed for other species, which are not shown here. This opposing effect of charge flow significantly reduces the total atomic charges on individual atoms than they would be anticipated from pure π delocalization. Consequently, it should be especially cautious to reach conclusions regarding resonance effects based on atomic charge variations.[5]

In the 90° rotamer structure, the localization scheme used in the present BLW treatment allows us to specifically visualize contributions from the "positive" and "negative" hyperconju-

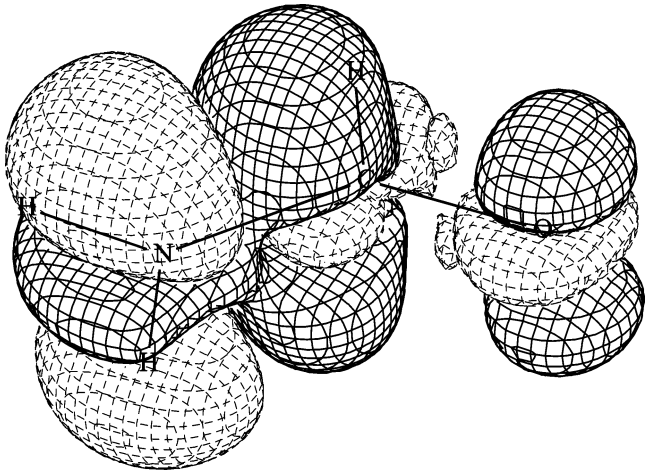

Figure 2. Electron density difference (EDD) map for the n−π resonance delocalization in the planar ground state of formamide. The contour level is 2×10^{-3} e/Bohr^3.

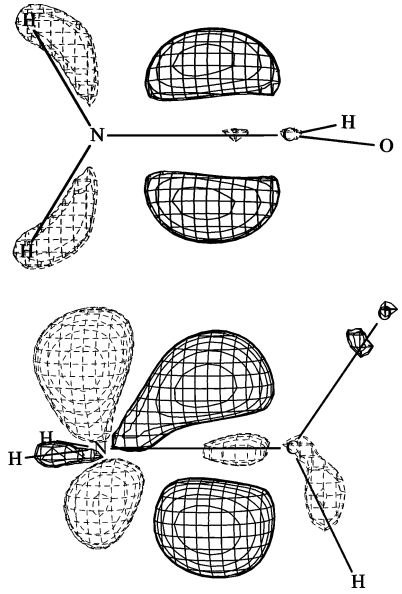

Figure 3. Electron density difference (EDD) map for the 90° rotamer structure of formamide, showing (a, top panel) $\pi_{NH_2} \rightarrow \pi^*_{C=O}$ hyperconjugation charge delocalization and (b, bottom panel) $n_N \rightarrow \sigma^*_{C=O}$ negative hyperconjugation interactions. The contour level is 2×10^{-3} e/Bohr^3.

gation effect. Shown in Figure 3 are the EDD plots for formamide due to the $\pi_{NH_2} \rightarrow \pi^*_{C=O}$ hyperconjugation (top) and the $n_N \rightarrow \sigma^*_{C=O}$ negative hyperconjugation interactions (bottom). It is important to notice that the hyperconjugation delocalization occurs primarily in the bonding region involving the interacting orbitals. The $\pi_{NH_2} \rightarrow \pi^*_{C=O}$ hyperconjugation reduces the charge density of the NH_2 group and enhances the electron density along the C−N bond. For the $n_N \rightarrow \sigma^*_{C=O}$ negative hyperconjugation, the same trend is observed, although the charge depletion is from the lone-pair orbital of nitrogen. The π symmetry in these hyperconjugation interactions is nicely reflected in the EDD plots. Importantly, these qualitative drawings suggest that the hyperconjugation effects are mainly local events of the molecular fragments involved, though they can still make significant energetic contributions as in π conjugations (Tables 1 and 4).

An approximate linear relationship was found (Figure 4) between the delocalization energy (ΔE_R) and the amount of

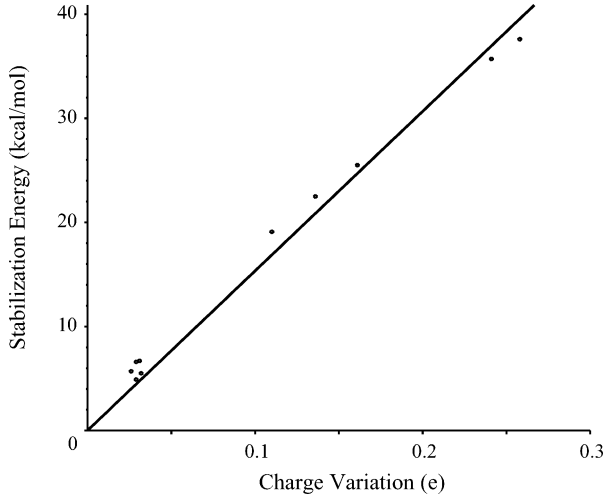

Figure 4. Correlation between computed resonance stabilization energy and the amount of charge migration from the nitrogen lone pair to the $\pi^*_{C=X}$ orbital.

charge migration from the localized nitrogen lone pair, $\Delta P_\pi(N)$:

$$\Delta E_R = k\Delta P_\pi(N) \tag{9}$$

where $\Delta P_\pi(N)$ is the difference in natural population of the nitrogen lone pair orbital between the Ψ^{HF} and Ψ^{BLW} wave functions. In eq 9, the slope k is found to be 154 kcal/mol per electron. To understand this apparent relationship, we show in Appendix B that eq 9 can be rationalized by the interaction between the n_N orbital and the virtual $\pi^*_{C=X}$ orbital. The constant, k, is related to the energy difference between the $\pi^*_{C=X}$ and n_N orbital, $k = \epsilon(\pi^*_{C=X}) - \epsilon(n_N)$. The linear relationship stems from the fact that $|\epsilon(n_N)|$ is much greater than $|\epsilon(\pi^*_{CX})|$. Consequently, k is dominated by $|\epsilon(n_N)|$.

Conclusions

In the present study, the rotational barriers in $HCXNH_2$ (X = O, NH, CH_2, S, and Se,) are decomposed into various energy components, including resonance conjugation energy, σ-framework steric effects, hyperconjugation energy, and pyramidization energy, using a block-localized wave function method with the 6-31G(d) basis set. This decomposition scheme, although not unique, makes it possible to investigate the important role of the electronic delocalization in determining the rotational barrier. The ground-state electronic delocalization, represented by resonance structure **3**, makes the largest contribution to the torsional barrier about the C−N bond, though the gain in hyperconjugation stabilization of the 90° rotamer structure reduces the overall delocalization effects. Steric effects due to conformational change in the σ framework and amino group pyramidization are also important in determining the barrier height of these compounds. The difference in torsional barrier in the chalcogen series, $HCXNH_2$ (X = O, S, and Se), primarily results from the difference in electronic delocalization of the ground-state structure, which is significantly greater for X = S and Se than X = O.

On the other hand, π resonance effects are smaller for X = NH and CH_2 in comparison with formamide. Therefore, the loss of the ground-state resonance stabilization results in lowering of the barrier height by about 3 and 6 kcal/mol for HC═NH-(NH_2) and HC═CH_2(NH_2). Hyperconjugation effects for the rotamer structures of X = O, NH, and CH_2 are similar and thus

do not contribute significantly to the overall difference in torsional barrier. In contrary to the chalcogen series, steric effects in the σ framework rotation are found to provide nearly equal or greater contributions to the reduction of the barrier height. Consequently, both ground-state π resonance and σ steric effects are critical in determining the amide rotational barrier, suggesting that torsional barrier itself is not a good measure of the π conjugation.[32]

We also performed ab initio VB calculations with all six conventional resonance structures for planar formamide, where the one-electron orbitals are pure atomic orbitals. The results reveal that the Lewis structures **1** and **2** make the largest contributions. The total structural weight of Lewis structures **3** and **4** is significant (ca. 20%). These structures are mainly responsible for the π electronic delocalization between the nitrogen lone pair and the π component of the C═X double bond.

Electron density difference (EDD) plots between the adiabatic structure and diabatic "valence bond" states makes it possible to visualize the origin of the electronic delocalization within each molecule. Of interest is the observation that the π electron flow from the nitrogen lone pair into the π_{CO}* orbital is concomitantly accompanied by the opposing migration of the σ charge density. Consequently, the change in integrated partial atomic charges based upon population or atom-in-molecule analysis is significantly reduced compared to that expected from pure π conjugation. The EDD maps also reveal that the charge flow due to hyperconjugation interactions occurs primarily in local regions.

Acknowledgment. This work was partially supported by the Western Michigan Univesity, National Natural Science Foundation of China, the Provincial Natural Science Foundation of Fujian, the Funds der Chemischen Industry (at Erlangen, PvRS), and the National Institutes of Health (J.G.).

Appendix A

The ab initio VB calculations were performed by a spin-free VB method, namely, the bonded tableau unitary group approach (BTUGA).[15,18] In the BTUGA, a VB function is defined as

$$\psi(k) = A_k e_{11}^{[\lambda]} \psi_0(k) = A_k e^{[\lambda]}{}_{11}[u_1^k(1)\, u_2^k(2) \ldots u_N^k(N)] \qquad \text{(A1)}$$

where A_k is a normalization constant, $e_{11}^{[\lambda]}$ is a standard projection operator, and u_i^k is a one-electron basis function. Also, if the spin quantum number of the system is S, $[\lambda] = [2^{(N/2)-S}, 1^{2S}]$ is an irreducible representation of permutation group S_N. In fact, the above VB function, which is equivalent to the famous Heitler−London−Slater−Pauling (HLSP) function, corresponds to a VB resonance structure where two one-electron basis u_{2i-1}^k and u_{2i}^k overlap to form a bond ($i \leq N/2 - S$ and if $u_{2i-1}^k = u_{2i}^k$ the "bond" is a lone electron pair) and the last $2S$ one-electron functions are unpaired (in the present cases $S = 0$). Thus the true wave function of the system can be expressed as a superimposition of all canonical VB functions (or resonance structures), namely

$$\Psi = \sum_{k=1}^{M} C_k \psi(k) \qquad \text{(A2)}$$

The structural weight of a VB function $\psi(k)$ is defined as

$$T_k = \sum_{l=1}^{M} C_k C_l S_{kl} \qquad \text{(A3)}$$

where S_{kl} is the overlap integral between the VB functions $\psi(k)$ and $\psi(l)$. The condition of normalization requires

$$\sum_{k=1}^{M} T_k = 1 \qquad \text{(A4)}$$

The VB calculations are performed for the conjugated π electrons and orbitals. The orbitals for the σ-framework are treated at the Hartree−Fock level, which are orthogonal to the π orbitals. In the present ab initio VB calculations, the σ-framework molecular orbitals are optimized simultaneously with the π VB orbitals and the coefficients of the resonance structures.

Appendix B

The delocalization energy due to the charge-transfer from the nitrogen lone pair to an adjacent virtual orbital can be generally described by the interaction between an occupied orbital φ_a and a virtual orbital φ_b; those energies are ϵ_a and ϵ_b, respectively.

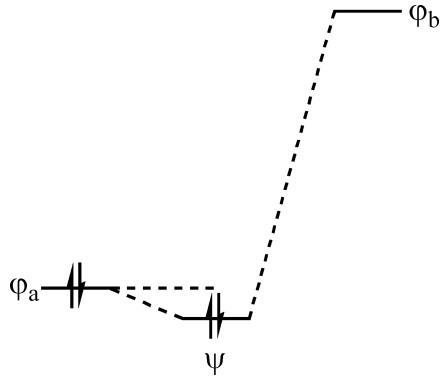

The interaction between φ_a and φ_b results in the occupied MO $\psi = \varphi_a + \lambda\varphi_b$ (note φ_a and φ_b are generally not orthogonal and their overlap and the Hamiltonian integrals are labeled as S_{ab} and H_{ab}), whose energy is E. For simplicity we use Mulliken population analysis, which is very close to the NAO results in this work, to compute the atomic populations. Thus, the amount of charges shifted from φ_a to φ_b is

$$\Delta P_\pi(N) = 2\frac{\lambda S_{ab} + \lambda^2}{1 + 2\lambda S_{ab} + \lambda^2} \qquad \text{(B1)}$$

and the stabilization energy (ΔE_R) is

$$\Delta E_R = 2(E - \epsilon_a) = 2\frac{\lambda^2(\epsilon_a - \epsilon_b)}{1 + 2\lambda S_{ab} + \lambda^2} \qquad \text{(B2)}$$

where the coefficient λ can be determined with a perturbation theory by noting that λ is a very small quantity:

$$\lambda = \frac{H_{ab} - \epsilon_a S_{ab}}{(\epsilon_a - \epsilon_b)} \qquad \text{(B3)}$$

The comparison between eqs B1 and B2 leads to

$$\Delta P_\pi(N) = \Delta E_R \frac{S_{ab} + \lambda}{\lambda(\epsilon_a - \epsilon_b)} \qquad \text{(B4)}$$

In the case that φ_a and φ_b are orthogonal, the above equation will be simplified to[33]

$$\Delta P_{\pi}(N) = \frac{\Delta E_R}{\epsilon_a - \epsilon_b} \tag{B5}$$

Supporting Information Available: Discussion and tables of geometrical features and natural population analyses. This information is available free of charge via the Internet at http://pubs.acs.org.

References and Notes

(1) For example: (a) Tasaki, K.; Suter, U. W. *J. Phys. Chem.* **1988**, *92*, 5886. (b) Schnur, D. M.; Yuh, Y. H.; Dalton, D. R. *J. Org. Chem.* **1989**, *54*, 3779. (c) Li, Y.; Garrell, R. L.; Houk, K. N. *J. Am. Chem. Soc.* **1991**, *113*, 5896. (d) Tsuzuki, S.; Tanabe, K. *J. Chem. Soc., Perkin Trans. 2* **1991**, 1255. (e) Duffy, E. M.; Severance, D. L.; Jorgensen, W. L. *J. Am. Chem. Soc.* **1992**, *114*, 7535. (f) Gao, J. *J. Am. Chem. Soc.* **1993**, *115*, 2930. (g) Gao, J. *Proc. Indian Acad. Sci. (Chem. Sci.)* **1994**, *106*, 507.

(2) Pauling, L. *The Nature of the Chemical Bond*; Cornell University Press: Ithaca, NY, 1960. (b) Wheland, G. W. *Resonance in Organic Chemistry*; Wiley: New York, 1955.

(3) Streitwieser, A.; Heathcock, C. H.; Kosower, E. M. *Introduction to Organic Chemistry*; Macmillan: New York, 1992.

(4) Bader, R. F. W. *Atoms in Molecules: A Quantum Theory*; Oxford University Press: Oxford, U.K., 1990.

(5) Wiberg, K. B. *Acc. Chem. Res.* **1999**, *32*, 922.

(6) Wiberg, K. B.; Breneman, C. M. *J. Am. Chem. Soc.* **1992**, *114*, 831. (b) Wiberg, K. B.; Hadad, C. M.; Rablen, P. R.; Cioslowski, J. *J. Am. Chem. Soc.* **1992**, *114*, 8644.

(7) Wiberg, K. B.; Rablen, P. R. *J. Am. Chem. Soc.* **1995**, *117*, 2201.

(8) Knight, E. T.; Allen, L. C. *J. Am. Chem. Soc.* **1995**, *117*, 4401.

(9) Laidig, K. E.; Cameron, L. M. *Can. J. Chem.* **1993**, *71*, 872.

(10) Laidig, K. E.; Cameron, L. M. *J. Am. Chem. Soc.* **1996**, *118*, 1737.

(11) Fogarasi, G.; Szalay, P. G. *J. Phys. Chem. A* **1997**, *101*, 1400.

(12) Glengening, E. D.; Hrabal, J. A., II. *J. Am. Chem. Soc.* **1997**, *119*, 12940.

(13) Weinhold, F.; Carpenter, J. E. *The Structure of Small Molecules and Ions*; Plenum Press: New York, 1988; p 227. (b) Glendening, E. D.; Reed, A. E.; Carpenter, J. E.; Weinhold, F. NBO Version 3.1.

(14) Lauvergnat, D.; Hiberty, P. C. *J. Am. Chem. Soc.* **1997**, *119*, 9478.

(15) Mo, Y.; Wu, W.; Zhang, Q. *J. Phys. Chem.* **1994**, *98*, 10048. (b) Mo, Y.; Wu, W.; Zhang, Q. *J. Mol. Struct. (THEOCHEM)* **1994**, *315*, 173. (c) Mo, Y.; Zhang, Q. *Int. J. Quantum Chem.* **1995**, *56*, 19. (d) Mo, Y.; Lin, Z.; Wu, W.; Zhang, Q. *J. Phys. Chem.* **1996**, *100*, 6469. (e) Mo, Y.; Lin, Z.; Wu, W.; Zhang, Q. *J. Phys. Chem.* **1996**, *100*, 11569.

(16) Hiberty, P. C.; Byrman, C. P. *J. Am. Chem. Soc.* **1995**, *117*, 9875.

(17) Mo, Y.; Peyerimhoff, S. D. *J. Chem. Phys.* **1998**, *109*, 1687. (b) Mo, Y.; Zhang, Y.; Gao, J. *J. Am. Chem. Soc.* **1999**, *121*, 5737. (c) Mo, Y.; Gao, J.; Peyerimhoff, S. D. *J. Chem. Phys.* **2000**, *112*, 5530.

(18) Zhang, Q.; Li, X. *J. Mol. Struct. (THEOCHEM)* **1989**, *198*, 413. (b) Li, X.; Zhang, Q. *Int. J. Quantum Chem.* **1989**, *36*, 599. (c) Wu, W.; Mo, Y.; Zhang, Q. *J. Mol. Struct. (THEOCHEM)* **1993**, *283*, 227. (d) Wu, W.; Wu, A.; Mo, Y.; Lin, M.; Zhang, Q. *Int. J. Quantum Chem.* **1998**, *67*, 287.

(19) Cooper, D. L.; Thorsteinsson, T.; Gerratt, J. *Adv. Quantum Chem.* **1999**, *32*, 51. (b) Karadakov, P. B.; Cooper, D. L.; Gerratt, J. *J. Am. Chem. Soc.* **1998**, *120*, 3975. (c) Gerratt, J.; Cooper, D. L.; Karadakov, P. B.; Raimondi, M. *Chem. Soc. Rev.* **1997**, *26*, 87. (d) Cooper, D. L.; Gerratt, J.; Raimondi, M. *Chem. Rev.* **1991**, *91*, 929. (e) McWeeny, R. *Int. J. Quantum Chem.* **1988**, *34*, 25. (f) McWeeny, R. *Pure Appl. Chem.* **1989**, *61*, 2087. (g) McWeeny, R. *J. Mol. Struct. (THEOCHEM)* **1991**, *229*, 29. (h) Shurki, A.; Hiberty, P. C.; Shaik, S. *J. Am. Chem. Soc.* **1999**, *121*, 822. (i) Mestres, J.; Hiberty, P. C. *New J. Chem.* **1996**, *20*, 1213. (j) Lauvergnat, D.; Hiberty, P. C.; Danovich, D.; Shaik, S. *J. Phys. Chem.* **1996**, *100*, 5715. (k) Hiberty, P. C. *J. Mol. Struct. (THEOCHEM)* **1998**, *451*, 237.

(20) Basch, H.; Hoz, S. *Chem. Phys. Lett.* **1998**, *294*, 117.

(21) March, J. *Advanced Organic Chemistry: Reactions, Mechanisms, and Structures*; Wiley: New York, 1992. (b) Loewenstein, A.; Melera, A.; Rigny, P.; Walter, W. *J. Phys. Chem.* **1964**, *68*, 1597. (c) Neuman, R. C., Jr.; Young, L. B. *J. Phys. Chem.* **1965**, *69*, 2570. (d) Sandstrom, J. *J. Phys. Chem.* **1967**, *71*, 2318. (e) Stewart, W. E.; Siddall, T. H., III. *Chem. Rev.* **1979**, *79*, 517. (f) Ou, M.-C.; Tsai, M.-S.; Chu, S.-Y. *J. Mol. Struct.* **1994**, *310*, 247.

(22) Prasad, B. V.; Uppal, P.; Bassi, P. S. *Chem. Phys. Lett.* **1997**, *276*, 31.

(23) Frisch, M. J.; Trucks, G. W.; Schlegel, H. B.; Gill, P. M. W.; Johnson, B. G.; Robb, M. A.; Cheeseman, J. R.; Keith, T.; Petersson, G. A.; Montgomery, J. A.; Raghavachari, K.; Al-Laham, M. A.; Zakrzewski, V. G.; Ortiz, J. V.; Foresman, J. B.; Cioslowski, J.; Stefanov, B. B.; Nanayakkara, A.; Challacombe, M.; Peng, C. Y.; Ayala, P. Y.; Chen, W.; Wong, M. W.; Andres, J. L.; Replogle, E. S.; Gomperts, R.; Martin, R. L.; Fox, D. J.; Binkley, J. S.; Defrees, D. J.; Baker, J.; Stewart, J. P.; Head-Gordon, M.; Gonzalez, C.; Pople, J. A. Gaussian; Gaussian, Inc.: Pittsburgh, PA, 1995.

(24) Mo, Y.; Lin, Z. *J. Chem. Phys.* **1996**, *105*, 1046. (b) Mo, Y.; Schleyer, P.v. R.; Jiao, H.; Lin, Z. *Chem. Phys. Lett.* **1997**, *280*, 439. (c) Minyaev, R. M.; Quapp, W.; Subramanian, G.; Schleyer, P.v. R.; Mo, Y. *J. Comput. Chem.* **1997**, *18*, 1792. (d) Mo, Y.; Jiao, H.; Lin, Z.; Schleyer, P. v. R. *Chem. Phys. Lett.* **1997**, *289*, 383. (e) Mo, Y.; Lin, M.; Wu, W.; Zhang, Q.; Schleyer, P.v. R. *Sci. China* **1999**, *42*, 253.

(25) Daudey, J. P.; Trinquier, G.; Barthelat, J. C.; Malrieu, J. P. *Tetrahedron* **1980**, *36*, 3399. (b) Mo, Y.; Lin, M.; Wu, W.; Zhang, Q. *Acta Chim. Sin.* **2000**, *58*, 218.

(26) Felgg, R. H.; Harcourt, R. D. *J. Mol. Struct. (THEOCHEM)* **1988**, *164*, 67.

(27) Glendening, E. D.; Badenhoop, J. K.; Weinhold, F. *J. Comput. Chem.* **1998**, *19*, 628.

(28) Hiberty, P. C.; Ohanessian, G. *J. Am. Chem. Soc.* **1982**, *104*, 66.

(29) Schleyer, P.v. R.; Kos, A. J. *Tetrahedron* **1983**, *39*, 1141. (b) Jemmis, E. D.; Schleyer, P. v. R. *J. Am. Chem. Soc.* **1982**, *104*, 4781. (c) Reed, A. E.; Schleyer, P. v. R. *J. Am. Chem. Soc.* **1987**, *109*, 7362. (d) Reed, A. E.; Schleyer, P. v. R. *J. Am. Chem. Soc.* **1990**, *112*, 1434. (e) Farnham, W. B.; Smart, B. E.; Middleton, W. J.; Calabrese, J. C.; Dixon, D. A. *J. Am. Chem. Soc.* **1985**, *107*, 4565. (f) Reed, A. E.; Schade, C.; Schleyer, P. v. R.; Kamath, P. V.; Chandrasekhar, J. *J. Chem. Soc., Chem. Commun.* **1988**, 67. (g) Salzner, U.; Schleyer, P. v. R. *J. Chem. Soc., Chem. Commun.* **1990**, 190. (h) Wiberg, K. B.; Rablen, P. R. *J. Am. Chem. Soc.* **1993**, *115*, 614.

(30) Wiberg, K. B.; Rablen, P. R. *J. Comput. Chem.* **1993**, *14*, 1504.

(31) Wiberg, K. B.; Hadad, C. M.; Breneman, C. M.; Laigig, K. E.; Murcko, M. A.; LePage, T. J. *Science* **1991**, *252*, 1266.

(32) Mo, Y.; Peyerimhoff, S. D. *Theor. Chem. Acc.* **1999**, *101*, 311.

(33) Reed, A. E.; Weinhold, F.; Curtiss, L. A. *Chem. Rev.* **1988**, *88*, 899.